Drug Design, Development and Therapy

Dovepress
Taylor & Francis Group

Open Access Full Text Article

ORIGINAL RESEARCH

Benzbromarone Analog SAR: Potent hURAT1 (SLC22A12) Inhibitors and Drug Transporter Interaction Studies

Promsuk Jutabha[1,2], Vijay Kumar[3], Naohiko Anzai[2,4], Peter J Rice[5,6], Janet W Lightner[6], Hitoshi Endou[7], Michael F Wempe[3,8,9]

[1]Chakri Naruebodindra Medical Institute, Faculty of Medicine Ramathibodi Hospital, Mahidol University, Samut Prakarn, 10540, Thailand; [2]Department of Pharmacology and Toxicology, Dokkyo Medical University School of Medicine, Tochigi, 321-0293, Japan; [3]Department of Sciences, School of Pharmacy, University of Colorado Denver Anschutz Medical Campus, Aurora, CO, 80045, USA; [4]Department of Pharmacology, Chiba University Graduate School of Medicine, Chiba, 260-8670, Japan; [5]Department of Clinical Pharmacy, School of Pharmacy, University of Colorado Anschutz Medical Campus, Aurora, CO, 80045, USA; [6]Department of Pharmacology, East Tennessee State University, Johnson City, TN, 37614, USA; [7]Department of Pharmacology and Toxicology, Kyorin University School of Medicine, Mitaka, 181-8611, Japan; [8]Department of Biological and Physical Sciences, Kentucky State University, Frankfort, KY, 40601, USA; [9]University of Colorado Cancer Center, University of Colorado Denver, Aurora, CO, 80045, USA

Correspondence: Michael F Wempe, Kentucky State University, 400 East Main St, Frankfort, KY, 40601, USA, Email Michael.Wempe@kysu.edu

Purpose: There were two main purposes for this study. One, to report two benzbromarone analogs and test their in vitro activity in the URAT1 inhibition assay; and two, to probe the structure–activity relationship (SAR) of various benzbromarone analogs regarding other drug transporters that may play a role in the uric acid uptake/elimination interplay.

Methods: In brief, chemical synthesis of two benzbromarone analogs was prepared using methods analogous to those reported. Furthermore, drug transporter protein inhibition was investigated in vitro using oocytes expressing hURAT1, hURATv1 (GLUT9), hOAT1, hOAT3, hOAT10, hNPT4, OATP1B1, OATP1B3 and OATP2B1 prepared and utilized to conduct inhibition studies. In addition, one novel benzbromarone analog was studied via in vivo rat pharmacokinetic experiments to determine apparent oral bioavailability.

Results: Two analogs, 6-fluoro-benzbromarone (**5**) and 5,6-difluoro-benzbromarone (**9**), were synthetically prepared and **5** had a hURAT1 IC_{50} inhibition of 18 ± 4 nM, while analog (**9**) had an IC_{50} of 245 ± 64 nM. Analog (**5**) had good oral bioavailability (F_a) >0.6 in rat. Eadie-Hofstee plot and double-reciprocal plot of the Michaelis–Menten equation are summarized for benzbromarone (**2**) and its major Phase I metabolite 6-hydroxy-benzbromarone (**3**).

Conclusion: These results illustrate that the K_m for [^{14}C]UA uptake was not altered in the presence of **2** or **3**, but rather the V_{max} was reduced in the presence of inhibitors when added to the uptake solutions. As a result, these data support the notion that **2** and **3** inhibit [^{14}C]UA uptake by non-competitive inhibition and not at the URAT1 binding site.

Keywords: oocyte transporter system, Eadie-Hofstee plot, rat pharmacokinetics, organic anion drug transporters

Introduction

Uric acid transporter 1 (URAT1; SLC22A12) was first reported in 2002 by Enomoto et al.[1] URAT1 is a member of the Organic Anion Transporter (OAT) family. URAT1 is present in renal proximal tubular cells and located on the apical membrane mediating uric acid re-absorption from the proximal tubule. Under normal conditions in adult humans, the uric acid (UA) level in men is below ~7 mg/dL while in females it is below ~6 mg/dL. When blood levels of UA are elevated, it is known as hyperuricemia and can lead to gout. Gout is a painful condition; a form of arthritis where elevated levels of UA have caused it to crystallize out of blood and usually initially presents itself in the foot, commonly in the big toe.[2] There are two classes of medications that are used to treat hyperuricemia: i) Uricosurics and ii) Xanthine Oxidase (XO) Inhibitors. XO inhibitors reduce the in vivo production of uric acid, whereas uricosurics increase UA excretion by reducing UA reabsorption after the kidneys have filtered the blood. There are several uricosuric agents provided in

Received: 26 June 2024
Accepted: 14 January 2025
Published: 26 February 2025

Table 1 Summary of Probenecid and Benzbromarone Analogs

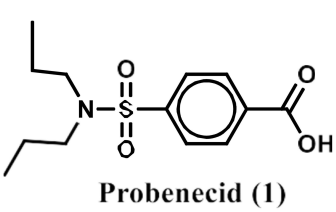

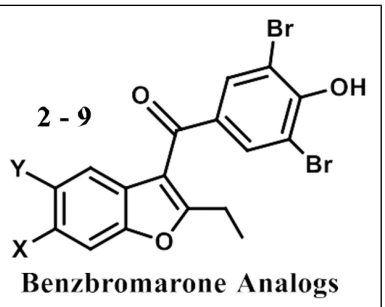

	Compound	X	Y	IC_{50} (nM)	SD	Fa
2	BEN	H	H	26	3	0.58
3	6-OH-BEN	OH	H	189	9	0.07
4	6-OMe-BEN	O-CH_3	H	111	14	0.13
5	6-F-BEN	F	H	18	4	0.64
6	5-OH-BEN	H	OH	138	9	0.25
7	5-OMe-BEN	H	O-CH_3	42	9	0.31
8	5-F-BEN	H	F	6	4	0.41
9	5,6-DiF-BEN	F	F	245	64	ND

Abbreviation: ND, No Bioavailability Data.

a recent review.[3] In the current work, probenecid (**1**) and benzbromarone analogs (**2**–**9**) were experimentally investigated (Table 1).

Benzbromarone is well known to be a hURAT1 inhibitor, with effective serum uric acid level lowering capacity. Benzbromarone can be hepatotoxic in patients consuming high amounts of alcohol daily.[4] Understanding the Structure–Activity Relationship (SAR) and transporter effects of benzbromarone analogs is important to elucidate. In fact, metabolic epoxidation of benzbromarone has been shown to be a critical step.[5] Previous work in our laboratories described the synthesis of several benzbromarone analogs and overall SAR. Compounds (**5**) and (**9**) were synthesized in 2011 (PCT/US2011/055006) and their activity reported herein for the first time.[6] We performed in vitro metabolism (Phase I and Phase II biotransformation) and in vivo pharmacokinetic experimentation in rats (ie, intravenous (iv) and oral dosing to determine bioavailability, F_a) and their uric acid inhibition were experimentally determined. As summarized in Table 1, benzbromarone (**2**), its major Phase I metabolite 6-hydroxy-benzbromarone (**3**), and various analogs (**3**–**9**) where position-X and -Y are different substituents; their corresponding in vitro IC_{50} values are reported. The methoxy analog of 3, 6-methoxy-benzbromarone (**4**) was previously prepared and tested. Analog (**5**), 6-fluoro-benzbromarone is disclosed herein. In contrast, the 5-hydroxy-benzbromarone (**6**), 5-methoxy-benzbromarone (**7**) and 5-fluoro-benzbromarone (**8**) analogs were previously prepared, and those in vitro and in vivo data are published. Lastly, the difluoro-analog (**9**) was also prepared in the current work; so, preparation and in vitro testing of (**5**) and (**9**) and the in vivo testing of (**5**) are reported herein. A goal of the SAR study was to be able to prepare benzbromarone analogs which block potential CYP catalyzed hydroxylation of benzbromarone with either a -OMe or -F group. In addition to these benzbromarone analogs, we also present several transporter experiments which compare probenecid and demonstrate additional differences in the benzbromarone transporter SAR.

Materials and Methods

Chemicals

p-Anisoyl chloride, benzophenone, boron tribromide, 2-bromo-4,5-difluorophenol, *N*-bromosuccinimide (NBS), *n*-butyllithium (1.6 M in cyclohexane), calcium chloride ($CaCl_2$), calcium nitrate ($Ca(NO_3)_2$), carbon disulfide (CS_2), chloroacetone, Collagenase type I from clostridium histolyticum, deuterated dimethyl sulfoxide (DMSO-d_6), deuterated-chloroform ($CDCl_3$), diethylene glycol (DEG), 3-fluorophenol, gentamicin, gluconate, hydrazine hydrate,

paraformaldehyde, probenecid, sodium dodecyl sulfate (SDS), sodium metal, sodium pyruvate, tin(IV) chloride, and uric acid, were procured from Sigma-Aldrich Chemical Company (St. Louis, MO). Acetone, anhydrous acetone, anhydrous acetonitrile, anhydrous sodium sulfate (Na_2SO_4), dichloromethane (DCM), hexanes, methanol, triethylamine (TEA), magnesium chloride, potassium carbonate (K_2CO_3), potassium chloride, ethyl acetate (EtOAc), hydrochloric acid (HCl), sodium bicarbonate ($NaHCO_3$), sodium chloride (NaCl), glucose, potassium chloride (KCl), sodium hydroxide (NaOH), potassium hydroxide (KOH), anhydrous $MgSO_4$, and tetrahydrofuran (THF) were purchased from Fisher Scientific (Pittsburgh, PA). Reactions were monitored via silica gel IB2-F thin-layer chromatography (TLC) plates from J.T. Baker (Phillipsburg, NJ). [^{14}C]Urate (55 mCi/mmol) was purchased from Moravek Inc. (Brea, CA, USA). *N*-(2-Hydroxyethyl)-piperazine-*N*′-(2-ethane sulfonic acid) (HEPES) was obtained from Dojindo Laboratories (Kumamoto, Japan). [^{3}H]Estrone sulfate (48.9 Ci/mmol) and [^{3}H]estradiol-17β-glucuronide (41.8 Ci/mmol) were procured from PerkinElmer (Waltham, MA, USA). Penicillin–streptomycin (10,000 units/mL and 10,000 mg/mL) was obtained from Nacalai Tesque, Inc. (Kyoto, Japan).

Oocyte Expression System and Inhibition Studies

Methods describing oocyte experiments have been previously published.[7] In summary, oocytes expressing hURAT1 (human Uric Acid Transporter 1; SLC22A12), hURATv1 (GLUT9; facilitated glucose transporter member 9; SLC2A9), hOAT1 (human Organic Anion Transporter 1; SLC22A6), hOAT3 (human Organic Anion Transporter 3; SLC22A8), hOAT10 (human Organic Anion Transporter 10; SLC22A13), hNPT4 (Human Sodium Phosphate Transporter 4; SLC17A3), OATP1B1 (Organic anion transporting polypeptide 1B1; SLCO1B1), OATP1B3 (Organic anion transporting polypeptide 1B3; SLCO1B3), and OATP1B1 (Organic anion transporting polypeptide 2B1; SLCO2B1) were prepared. As a summary, cRNA was synthesized using T7 RNA polymerase via message matching high yield capped RNA transcription kit (Ambion; Austin, TX, USA). cRNA polyadenylation at the 3′-end was conducted via poly(A) tailing kit (Ambion; Austin, TX, USA). Xenopus female frogs (African clawed frogs; 95–120 g) were purchased from Sato Zoushoku (Chiba, Japan) and nurtured in tap water (19 ± 3 °C). The animal protocol was approved by the Committee of Research Center for Animal Laboratory in Dokkyo Medical University, Japan.

Xenopus laevis oocytes (1.23 ± 0.11 mg/oocyte) were defolliculated with collagenase (1.0 mg/mL) in calcium-free solution comprising 96.0 mM NaCl, 1.0 mM $MgCl_2 \cdot 6H_2O$, 5.0 mM HEPES, 2.0 mM KCl, pH 7.5, incubated for 2.0 h. The defolliculated oocytes were washed (Ca^{+2} free solution) and transferred into ND96 buffer (1.0 mM $MgCl_2$, 1.0 mM $CaCl_2$, 2.0 mM KCl, 96.0 mM NaCl, 5.0 mM HEPES, pH 7.5). Stage IV and V oocytes were selected and incubated overnight at 18 ± 2 °C in ND96 buffer containing penicillin (100 units/mL), pyruvate (2.5 mM), gentamicin (50 mg/mL), and streptomycin (0.10 mg/mL). Using an automated cRNA injector developed by Hitachi Ltd. (Tokyo, Japan), viable oocytes were next injected with 25 ng of capped cRNA and incubated at 18 ± 2 °C for 2–3 days in ND96 solution (96 mM NaCl, 2.0 mM KCl, 1.0 mM $MgCl_2$, 1.8 mM $CaCl_2$, and 5.0 mM HEPES buffer, pH 7.4) containing sodium pyruvate (1.0 mM) and gentamicin (50 μg/mL). Next, at room temperature, uptake experiments were performed in ND96 or chloride free (for URAT1; Cl^- in the ND96 solution was replaced with gluconate) uptake solutions. Uptake experiments were conducted by replacing the initial solution with an uptake solution (150 μL) containing radiolabeled substrate with or without testing non-labelled compounds. After the incubation period, the oocytes were washed three times with ice-cold ND96 solution (250 μL) and then dissolved in 5% (w/v) SDS (100 μL). Solution and oocyte radioactivity were determined with liquid scintillation counter (LSC; Aloka 3100; Aloka Co., Ltd., Tokyo, Japan). For inhibition studies, inhibitors were either injected into oocytes with a substrate or merely added to the ND96 solution. For the trans-inhibition, test compound was injected (46 nL) into the oocyte. The compound injected oocytes were washed once with ND96 solution and then incubated with a radiolabeled substrate. After 60 min of incubation, the uptake was terminated by washing oocytes with ice-cold uptake solution (5 × 1.0 mL). Oocytes were then solubilized with SDS (5% w/v), and radioactivity content was determined by using LSC. Control oocyte radioactivity was subtracted from hURAT1 expressing oocytes. The radiolabeled substrates used in this study were [^{14}C]-uric acid for URAT1, URATv1, OAT1, OAT3, OAT10, and NPT4, and [^{3}H]-estrone sulfate for OATP1B1 and 2B1, while the substrate for 1B3 was [^{3}H]-estradiol-17β-glucuronide. All experiments (n = 5–6 oocytes per experiment) were performed three times (three different days via different batches of oocytes) to demonstrate reproducibility. Statistics were performed using GraphPad Prism

(graphpad.com). All the data were statistically analyzed using one-way ANOVA followed by a Tukey–Kramer comparison test. Values are reported as the mean ± S.D. The ANOVA was used to determine significant differences and a value of $P < 0.05$ was considered significant.

Xanthine Oxidase Inhibition Assay

In vitro xanthine oxidase (XO) assay was determined using a xanthine oxidase fluorometric assay kit (Cayman Chemical Company, Ann Arbor, MI). The inhibitory effect of compounds was performed by adding various concentrations of each compound to evaluate IC_{50} values. The assay was performed in triplicate and on different days to demonstrate reproducibility. The IC_{50} values are reported as the mean ± S.D.

Liquid Chromatography Mass-Spectrometry-Mass Spectrometry (LC/MS-MS)

An Applied Biosystems Sciex 4000 (Applied Biosystems, Foster City, CA) was attached to a Shimadzu HPLC (Shimadzu Scientific Instruments, Inc, Columbia, MD) and a LEAP auto-sampler (LEAP Technologies, Carrboro, NC). A Zorbax extended-C18 50 × 4.6 mm 5-micron column with a column guard was used at 40 °C, 0.4 mL/min. The mobile phase "A" was NH_4OAc (10 mm), formic acid (0.1%) in H_2O, and "B" was 1:1 ACN:MeOH. A gradient was used, and the chromatography method was 95% A for 0.5 min, ramped to 95% B at 4.5 min and held for 5.0 min, and, lastly, brought back to 95% A at 10.5 min and held for 1.5 min (12 min total run time). Synthesized compounds were monitored via electro-spray ionization negative ion mode (ESI-) using the following conditions: (i) an ion spray voltage of −4200 V; (ii) temperature 450°C; (iii) curtain gas (CUR; set at 10) and collisional activated dissociation (CAD; set at 12 and gas was nitrogen); (iv) ion source gas one (GS1) and two (GS2) were set at 30; (v) entrance potential was set at −10 V; (vi) quadruple one (Q1) and three (Q3) were set on unit resolution; (vii) dwell time was set at 200 msec; and (viii) declustering potential (DP), collision energy (CE), and collision cell exit potential (CXP) are voltages (V); CXP was set at −15. Samples (10 μL) were analyzed in duplicate by liquid chromatography/mass spectrometry-mass spectrometry (LC/MS-MS).

Rat Pharmacokinetic (PK) Experiments

The in vivo portion was conducted at Quillen College of Medicine (East Tennessee State University (ETSU); Johnson City, TN). The experiments were conducted in an Association for Assessment and Accreditation of Laboratory Animal Care International accredited facility. All procedures were reviewed and approved by the ETSU Committee on Animal Care. The research procedures adhered to the Principles of Laboratory Animal Care (National Institutes of Health publication No 85–23, revised in 1985). Adult male Sprague-Dawley rats were purchased from Harlan World Headquarters (Indianapolis, IN) and housed in groups of three at 22 °C ± 1 °C and 55% ± 15% humidity with 12-hr dark–light cycles. Dosing was conducted 2.0–3.0 hr after the beginning of a light cycle. All animals were in cages with bedding, and they had free access to water, but were fasted 12–15 hr prior to dosing. Fasted animals (286 ± 12 g) were dosed either (a) via capsule dosing using a Torpac capsule syringe (Torpac, Fairfield, NJ) immediately followed by a bolus of HPLC grade H_2O (500 μL); or, (b) ophthalmic venous plexus (orbital sinus dosing) using a 1.0 mL disposable syringe with a 27G needle. CMC (carboxymethylcellulose) formulation was prepared by weighing synthesized compound into a glass vial and adding four weight equivalents of CMC. A stir vane was added, capped, and stirred (4.0 hr). Thereafter, to help remove clumps or aggregates that might have formed while mixing, the materials were removed and passed through a 35-mesh sieve screen. After additional mixing, the blend containing approximately 20 weight percent drug and was used to prepare capsules. Using a filling funnel, the 6-fluoro-benzbromarone (5)/CMC formulation was encapsulated into hard shell Torpac Lock ring gel (size 9) capsules (Torpac). Intravenous doses administered through the ophthalmic venous plexus were prepared immediately prior to dosing as aqueous solutions containing 10% DMSO; these rats were anesthetized with isoflurane and subsequently infused (~300 μL over, 30 sec) with corresponding drug solution via the ophthalmic venous plexus (orbital sinus). Using tail-vein collection (the posterior portion was transected 2–3 mm), blood samples (125 μL) were collected using mini-capillary blood collection tubes containing EDTA dipotassium salt (SAFE-T-FILL®; RAM Scientific Inc, Yonkers, NY). Animals administered drug orally had blood samples taken at 0.5, 1.0, 1.5, 2.0, 3.0, 4.0, 5.0, 6.0, 7.0, 8.0, 12, 24 and 30 hr post-dose, whereas, intravenous (orbital

sinus dosing) had time points of 0.083, 0.25, 0.50, 0.75, 1.0, 1.5, 2.0, 2.5, 3.0, 4.0, 5.0, 6.0, 8.0 and 24 hr post-dose. Immediately after filling, individual sample tubes were mixed and placed on dry ice and kept frozen (−80 °C ± 10°C) until sample preparation and subsequent LC/MS-MS analysis. Control rat blood collected with K_2EDTA was purchased from Bio-reclamation LLC (Westbury, NY). The control blood was used to prepare standard curves in triplicate, which were used to compute apparent in vivo blood concentration. Standard curves (SC) were prepared by addition with thorough mixing of various aqueous solutions (100 µL) into control blood (900 µL) and then serial dilutions with control blood. Standards were mixed and immediately frozen (−80°C ± 10°C). Standard samples were extracted and processed in an analogous fashion as in vivo samples as follows: The pharmacokinetic sample tubes were removed from the freezer (−80°C ± 10°C) and allowed to thaw on ice (20–30 min). The tubes were vortex-mixed (4–5 s) followed by extraction solution (Solvent B containing benzbromarone (**2**) as an internal standard; 250 µL) addition, vortex-mixed (4–5 s) again, sat at RT for 5.0 min, vortex-mixed an additional time (4–5 s), and centrifuged at 11,000 rpm (10 min) using an Eppendorf mini-spin centrifuge (Hamburg, Germany). The supernatants were transferred into individual wells of a 96-well plate. The 96-well plate was placed into the LEAP auto-sampler cool-stack (8.0°C ± 0.1°C) and immediately analyzed via LC/MS-MS. Benzbromarone (2) t_R 6.1 – 6.2 min, 422.9 → 250.6 m/z, DP = −85, CE = −40; 6-fluoro-benzbromarone (**5**), t_R = 6.2 min, 458.9 → 250.8 m/z, DP = −85, CE = −44. 6-Fluoro-benzbromarone (**5**) rat blood standard curves were prepared (0.54–8841 ng/mL) with freeze-thaw cycle analogous to the in vivo samples producing a Limit-of-Detection (LOD) of 0.54 ng/mL and Limit-of-Quantitation (LOQ) of 1.08 ng/mL. The data were processed with a $1/X^2$ weighting and a non-linear fit with an R^2 of 0.986. The LC/MS-MS methods were validated with standard curves on three consecutive days, including quality control samples, performing freeze thaw stability study, etc.

Chemical Synthesis

Compound **5** was prepared according to Figure 1 starting from 2-fluoro-phenol.

4-fluorosalicaldehyde (**11**): To an oven-dried, 500 mL round-bottomed flask (RBF) equipped with a Teflon-coated magnetic stir bar (SB) and charged with 3-fluorophenol (**9**; 20.0 g, 178 mmol) in anhydrous acetonitrile (400 mL). The contents were cooled to 0 °C and magnesium chloride (51.0 g, 535 mmol) was added. Next, TEA (97.1 mL, 696 mmol) was added, stirred for 25 min and then paraformaldehyde (31.6 g, 696 mmol) was added. After the addition, the reaction mixture was refluxed for 3 h. The reaction was then cooled to ambient temperature, quenched with ice-cold concentrated

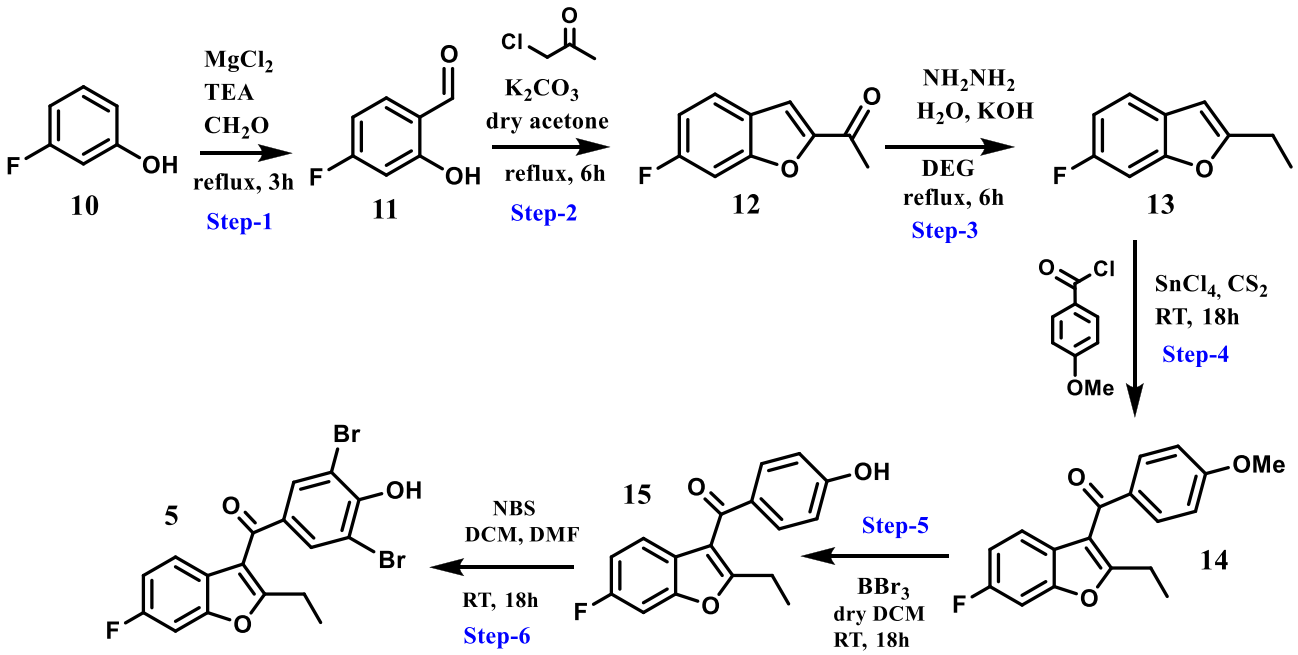

Figure 1 Preparation of 6-F-BEN, Compound **5**.

https://doi.org/10.2147/DDDT.S474398

hydrochloric acid and extracted with ethyl acetate. The organic layer was dried over Na_2SO_4, filtered, evaporated, and chromatographed over silica gel eluting with Hex-DCM-MeOH to afford **11** (12.0 g, 48% yield).

1-(6-fluorobenzofuran-2-yl)ethanone (12): To a dry RBF (250 mL) containing an SB, K_2CO_3 (18.02 g, 142.8 mmol) was diluted with anhydrous acetone (100 mL) and then stirred. Next, **11** (10.0 g, 71.4 mmol) was added dropwise (2–3 min) followed by chloro-acetone (6.32 mL, 78.5 mmol) addition (2–3 min). A reflux condenser was attached, and the contents were heated to reflux (6 h). The contents were cooled to ambient temperature and Büchner filtered; the solid was rinsed with acetone (2 × 100 mL). The filtrate was concentrated under reduced pressure and purified via SiO_2 chromatography (Hex-DCM) to afford a light-yellow solid, **12** (7.20 g, 57% yield). ^{1}H-NMR (DMSO-d_6, 400 MHz): ^{1}H NMR (DMSO-d_6, 400 MHz): δ ppm 7.66–7.62 (m, 1H), 7.47 (s, 1H), 7.28–7.25 (dd, 1H), 7.11–7.05 (m, 1H), and 2.58 (3, 3H).

2-ethyl-6-fluorobenzofuran (**13**): Compound **12** (3.00 g, 16.8 mmol) in an RBF/SB (250 mL) was mixed with DEG (100 mL) and heated (120–130 °C). The mixture was stirred and hydrazine hydrate (3.26 mL, 67.2 mmol) was added dropwise (5–10 min). The mixture was heated (180–190 °C,10 min) and then the temperature decreased to 120–130 °C. Next, KOH (3.77 g, 67.2 mmol) was carefully added in portions with heating (120–130 °C, 6 h). The contents were diluted with ice water (250 mL) and extracted (DCM, 4 × 100 mL). The organic phase was dried over anhydrous $MgSO_4$, filtered, concentrated under reduced pressure, and purified via SiO_2 chromatography (Hex-DCM) to afford **12** as a light-yellow oil (2.20 g, 80% yield).^{1}H-NMR (DMSO-d_6, 400 MHz): δ ppm 7.33–7.30 (m, 1H), 7.15–7.13 (m, 1H), 6.94–6.89 (m, 1H), 6.35 (s, 1H), 2.82–2.76 (q, 2H), 1.35–1.31 (t, 3H).

(2-ethyl-6-fluorobenzofuran-3-yl)(4-methoxyphenyl)methanone (**14**): An oven-dried RBF (500 mL), SB, and **13** (5.00 g, 30.5 mmol) was diluted with CS_2 (250 mL). The reaction vessel was capped with a sure-seal, and an N_2 balloon was attached. The RBF was cooled in an ice bath (30 min), and p-anisoyl chloride (5.40 mL, 39.7 mmol) was added dropwise (3–4 min). Next, tin(IV) chloride (4.64 mL, 39.7 mmol) was added. The mixture was warmed to room temperature and stirred (18 h). The contents were diluted (H_2O, 200 mL) and extracted with EtOAc (4 × 200 mL). The organic phase was washed with dilute HCl, followed by water, $NaHCO_3$(aq), and saturated NaCl(aq). The organic phase was dried ($MgSO_4$), filtered, concentrated under reduced pressure, and purified via SiO_2 chromatography (Hex-DCM) to afford 14 (4.50 g, 50% yield) as a white solid. ^{1}H NMR ($CDCl_3$, 400 MHz): δ ppm 7.85–7.80 (d, 2H), 7.37–7.33 (m, 1H), 7.20–7.17 (dd, 1H), 6.98–6.93 (m, 3H), 3.89 (s, 3H), 2.90–2.84 (q, 2H), 1.34–1.30 (t, 3H).

(2-ethyl-6-fluorobenzofuran-3-yl)(4-hydroxyphenyl)methanone (**15**): An oven-dried RBF (250 mL) equipped with a SB was charged with **14** (5.00 g, 16.8 mmol) in dry DCM (50 mL). The mixture was cooled using an ice bath. After 10 min, boron tribromide (2.39 mL, 25.1 mmol) was added and the reaction mixture was stirred (30 min). Next, the reaction mixture was stirred at room temperature for 18 h, then H_2O was added; the solution was neutralized with sat. sodium bicarbonate solution; and then extracted with DCM. The organic layer was dried over anhydrous Na_2SO_4, filtered, evaporated and chromatographed over silica gel eluting with Hex:DCM:MeOH (1:1:1) to afford **15** (3.10 g, 66% yield). ^{1}H NMR ($CDCl_3$, 400 MHz): δ ppm 7.80–7.76 (d, 2H), 7.37–7.33 (m, 1H), 7.21–7.18 (dd, 1H), 6.99–6.93 (m, 1H), 6.92–6.90 (d, 2H), 6.08 (s, 1H), 2.90–2.84 (q, 2H), 1.34–1.30 (t, 3H).

(3,5-dibromo-4-hydroxyphenyl)(2-ethyl-6-fluorobenzofuran-3-yl)methanone (**5**): In a 100 mL RBF with SB was added NBS (1.32 g, 7.39 mmol). Next, DCM (90 mL) was added followed by the addition of DMF (10 mL). The mixture was cooled in an ice/NaCl bath (10 min), and **15** (1.0 g, 3.52 mmol) in DCM (20 mL) added. The mixture was warmed to room temperature (18 h) and quenched with water (100 mL) and diluted with additional DCM (100 mL). The organic phase was washed with H_2O (100 mL) and then NaCl(aq) (100 mL). The organic phase was dried (anhydrous Na_2SO_4), filtered, concentrated under reduced pressure, and purified via SiO_2 chromatography (Hex:DCM:MeOH) to give **5** (600 mg, 39% yield) as an off-white solid. ^{1}H NMR ($CDCl_3$, 400 MHz): δ ppm 7.97 (s, 2H), 7.40–7.36 (m, 1H), 7.23–7.20 (dd, 1H), 7.04–6.99 (m, 1H), 6.32 (s, 1H), 2.89–2.82 (q, 2H), 1.37–1.32 (t, 3H). ^{13}C NMR ($CDCl_3$, 100 MHz): δ ppm 187.5 (CO), 167.7 (C), 162.0 (C), 159.6 (C), 153.7 (C), 153.2 (C), 133.5 (CH), 122.9 (C), 121.5 (CH), 115.2 (C), 112.2 (CH), 110.1 (CH), 99.2 (CH), 22.0 (CH_2), 11.2 (CH_3).

Compound **9** was prepared according to Figure 2 starting from 2-bromo-4,5-difluorophenol. The synthesis of **9** was prepared in six steps.

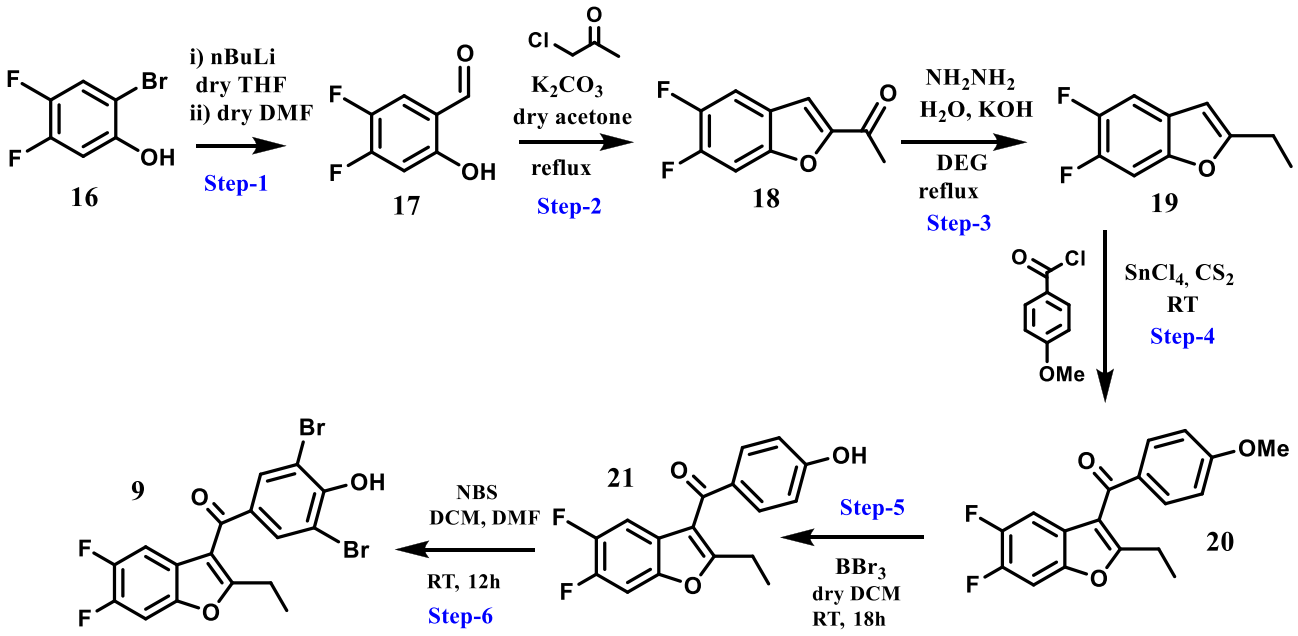

Figure 2 Preparation of 5.6-diF-BEN, compound **9**.

4.5-difluoro-2-hydroxybenzaldehyde (**17**). To a solution of 2-bromo-4,5-difluorophenol (**16**; 5.00 g, 23.9 mmol) in anhydrous tetrahydrofuran (500 mL; freshly prepared over sodium/benzophenone), was cooled with a dry ice acetone bath (–78 °C) with a nitrogen balloon attached. Upon cooling (20–30 min), *n*-butyllithium (1.6 M in cyclohexane, 37.4 mL, 59.8 mmol) was added dropwise via syringe transfer. The mixture was stirred at –78 °C for 30 min, at which time DMF (4.61 mL, 59.8 mmol) was added. The reaction mixture was allowed to slowly warm and then stirred at room temperature for 18 h. Water was added to the mixture (200 mL), and the solution was concentrated in vacuo. The residue was acidified with excess hydrochloric acid (2.0 M) and extracted with EtOAc (2 × 200 mL). The combined organic extracts were dried over anhydrous $MgSO_4$ and filtered and purified by silica gel column (9:1, Hex:EtOAc) to afford **17** (1.01 g, 27% yield). ^{1}H NMR (400 MHz) $CDCl_3$: 11.15 (s, 1H), 9.78 (s, 1H), 7.39–7.33 (m, 1H), 6.82–6.76 (m, 1H).

1-(5,6-difluorobenzofuran-2-yl)ethanone (**18**). To a solution of **17** (500 mg, 3.16 mmol) in dry acetone was added K_2CO_3 (1.74 g, 12.6 mmol). Next, chloroacetone (3.10 mL, 3.79 mmol) was added dropwise (2 to 3 min). A reflux condenser was attached, and the contents were heated to reflux for 24 h. The contents were cooled to ambient temperature and filtered via Büchner filtration. The solid was rinsed with acetone (2 × 100 mL). The filtrate was concentrated under reduced pressure and then purified via silica gel chromatography (9:1, Hex:EtOAc) to afford **18** as a white solid (250 mg, 40% yield). ^{1}H NMR (400 MHz) $CDCl_3$: 7.51–7.44 (m, 2H), 7.43–7.37 (m, 1H), 2.56 (s, 3H).

2-ethyl-5,6-difluorobenzofuran (**19**). Compound **18** (1.00 g, 5.09 mmol) in an RBF (250 mL) containing an SB was mixed with diethylene glycol (DEG; 100 mL) and heated to 120 °C. The mixture was stirred, and hydrazine hydrate (1.33 mL, 55% aqueous solution) was added dropwise (15–20 min) at 120 °C. After the addition, the mixture was heated to 180 °C for 10 min and cooled back to 120–130 °C. Next, KOH (1.08 g) was carefully added in portions and heated (120–130 °C for 6 h). The contents were diluted with ice water (220–230 mL) and extracted with DCM (4 × 50 mL). The organic phase was dried over anhydrous $MgSO_4$, filtered, concentrated under reduced pressure, and purified via silica gel chromatography (9:1, Hex:EtOAc) to afford **19** (601 mg, 65% yield). ^{1}H NMR (400 MHz) $CDCl_3$: 7.25–7.18 (m, 2H), 6.31 (s, 1H), 2.82–2.73 (m, 2H), 1.34–1.28 (m, 3H).

(2-ethyl-5,6-difluorobenzofuran-3-yl)(4-methoxyphenyl)methanone (**20**). To **19** (1.30 g, 7.13 mmol) in an RBF (250 mL) and SB was diluted with CS_2 (100 mL). The reaction vessel was capped with a sure-seal, and a N_2 balloon was attached. The RBF was cooled in an ice bath (30 min), and *p*-anisoyl chloride (1.3 mol equiv) was added dropwise (3 to 4 min); next, tin(IV) chloride (1.3 mol equiv) was added dropwise (5 to 7 min), and the mixture was stirred at 70 °C for 36 h. The contents were then diluted with H_2O (40 mL) and extracted with EtOAc (4 × 150 mL). The organic phase

https://doi.org/10.2147/DDDT.S474398

was washed with dilute HCl (0.5 N, 75 mL), followed by H_2O (75 mL), 1.0 M NaOH(aq) (75 mL), $NaHCO_3$(aq) (75 mL), and NaCl(aq) (75 mL). The organic phase was dried over anhydrous $MgSO_4$, filtered, concentrated under reduced pressure, and purified via silica gel chromatography (10:1, Hex:EtOAc) to afford **20** (501 mg, 22% yield). ^{1}H NMR (400 MHz) $CDCl_3$: 7.80 (d, *J* = 8 hz, 2H), 7.32–7.28 (m, 1H), 7.24–7.19 (m, 1H), 6.97 (d, *J* = 8 hz, 2H), 3.91 (s, 3H), 2.89–2.83 (m, 2H), 1.33–1.29 (m, 3H).

(2-ethyl-5,6-difluorobenzofuran-3-yl)(4-hydroxyphenyl)methanone (**21**). To **20** (800 mg, 2.52 mmol) in an RBF (250 mL) and SB was diluted with dry DCM (150 mL). The reaction vessel was capped with a sure-seal, and a N_2 balloon was attached. The RBF was cooled in an ice bath (30 min), and BBr_3 (0.36 mL, 3.79 mmol) was added dropwise (3 to 4 min). The reaction mixture was stirred at room temperature for 16 h. Next, H_2O was added, and the solution was extracted with DCM. The organic layer was dried over anhydrous Na_2SO_4, filtered, evaporated and chromatographed over silica gel eluting with DCM:MeOH (99:1) to afford **21** (601 mg, 79% yield). ^{1}H NMR (400 MHz) $CDCl_3$: 7.78–7.75 (m, 2H), 7.32–7.28 (m, 1H), 7.24–7.19 (m, 1H), 6.93–6.90 (m, 2H), 5.60 (s, 1H), 2.89–2.83 (m, 2H), 1.33–1.29 (m, 3H).

(3,5-dibromo-4-hydroxy-phenyl)-(2-ethyl-5,6-difluorobenzofuran-3-yl)methanone (**9**). In a RBF (100 mL) with an SB, NBS (0.37 g, 2.1 mmol) in DCM (50 mL) was added. Next, DMF (0.5 mL) was added, and the mixture cooled in an ice bath (20 min). Next, compound **21** (300 mg, 0.99 mmol) in DCM (0.5 mL) was added and warmed to room temperature (16 h). The reaction mixture was quenched with H_2O and washed with NaCl(aq). The organic phase was dried over Na_2SO_4, filtered, concentrated under reduced pressure, and purified via SiO_2 chromatography (Hex:EtOAc, 4:1) to afford **9** (95 mg, 21% yield) as an off-white solid. ^{1}H NMR (400 MHz) $CDCl_3$: 7.95 (s, 2H), 7.34–7.26 (m, 2H), 6.41 (s, 1H), 2.86–2.79 (m, 2H), 1.35–1.29 (m, 3H).

Results

hURAT1 Transporter Expressing Oocytes

The hURAT1 expressing oocytes provided in vitro IC_{50} values for hURAT1 inhibitors **5** and **9** and related benzbromarone analogs, summarized in Table 1. Compound **5**, 6-fluoro-benzbromarone, was more potent than the 5.6-difluoro-analog **9**. From the entire SAR list, the potency rank (most to least potent) order was **8** > **5** > **2** > **7** > **4** > **6** > **3** > **9**. Hence, two compounds (**8** and **5**) display a lower in vitro IC_{50} than parent benzbromarone **2**. Uric acid is a substrate for several renal tubular cell transporters, major players are depicted in Figure 3. Apical (brush border membrane) transporters include URAT1 (Uric acid transporter 1; SLC22A12), OAT10 (Organic Anion Transporter 10; SLC22A13) and NPT4 (hOATv1; SLC17A3); whereas the basolateral transporters include Glut9 (Glucose Transporter 9; URATv1), OAT1 (Organic Anion Transporter 1; SLC22A6) and OAT3 (Organic Anion Transporter 3; SLC22A8).

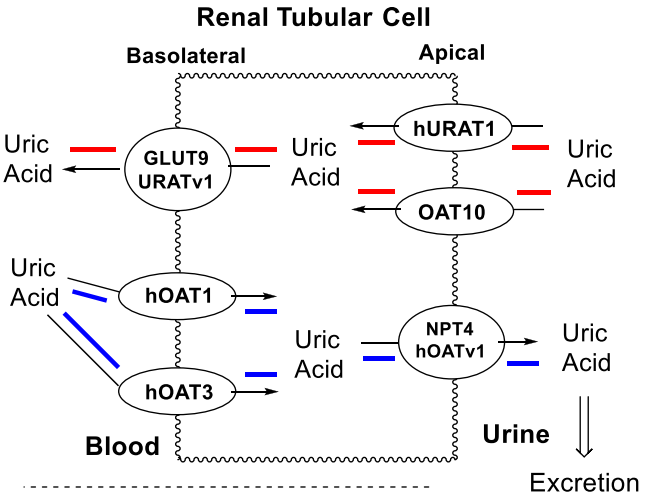

Figure 3 Summary of uric acid excretion and absorption pathways.

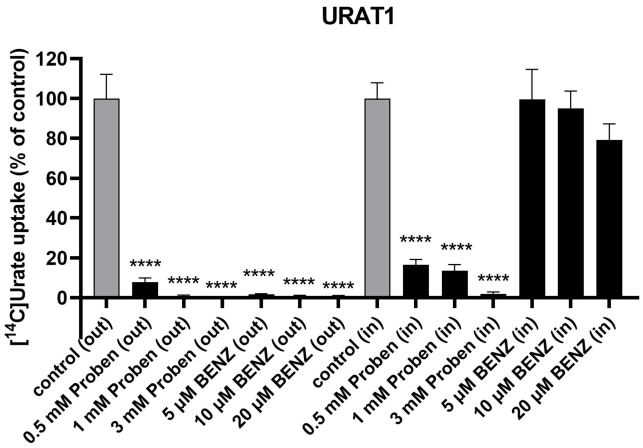

Figure 4 hURAT1 expressing oocytes and urate transport in the presence of either inside or outside probenecid or benzbromarone. ****P<0.0001 vs control, n = 6.

Utilizing hURAT1 expressing oocytes, when [^{14}C]UA (10 µM) was incubated in the presence of probenecid (*ie,* 500, 1000 and 3000 µM) or benzbromarone (5.0, 10 and 20 µM) both compounds displayed potent urate transport inhibition with benzbromarone being much more potent than probenecid as depicted in Figure 4. From these data, interesting observations may be concluded; for example, both probenecid and benzbromarone applied in the uptake solution statistically reduced the uptake of [^{14}C]UA. In contrast, when the inhibitors were injected inside the oocyte, probenecid but not benzbromarone inhibited [^{14}C]UA uptake. This illustrates the site specificity of benzbromarone as a UA uptake inhibitor; translating that the inhibition of UA uptake via benzbromarone (analogs) occurs at the urine-apical membrane interface.

hOAT10 Expressing Oocytes

Analogous experiments were conducted with hOAT10 expressing oocytes. Probenecid in the uptake solution displayed (Figure 5) potent inhibition of [^{14}C]UA uptake, while benzbromarone in the uptake solution displayed weak OAT10 inhibition of [^{14}C]UA uptake. In contrast, when these compounds were injected inside the oocytes, probenecid displayed weak [^{14}C]UA uptake inhibition, while benzbromarone did not produce a statistically different uptake as compared to control. Interesting to mention that the metabolite of benzbromarone (**2**) to 6-hydroxybenzbromarone (**3**) had the lowest IC_{50} (3.7 µM; Table 2), while analog **5** had the highest IC50 value (39.6 µM). The analogs ranged in their IC_{50} values (3.7–39.6 µM).

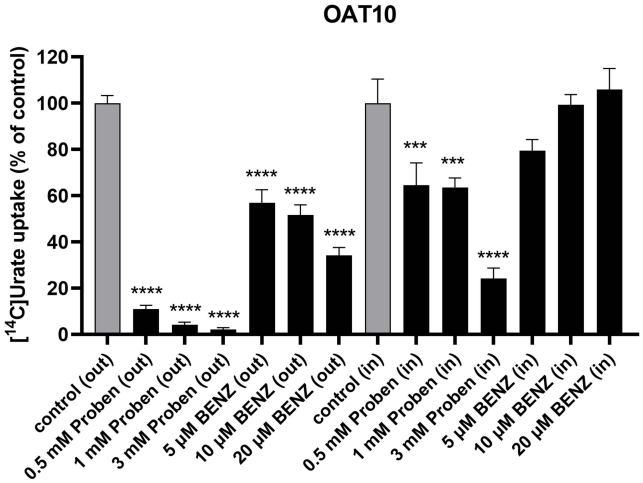

Figure 5 hOAT10 expressing oocytes and urate transport in the presence of either inside or outside probenecid or benzbromarone. ***P<0.001, ****P<0.0001 vs control, n = 6.

https://doi.org/10.2147/DDDT.S474398

Table 2 Summary of Benzbromarone Analog IC_{50} Values for hURAT1, hOAT10, hURATv1 (GLUT9), Xanthine Oxidase, OATP's 1B1, 1B3 and 2B1

	BEN Compound	hURAT1		hOAT10		hURATv1 (GLUT9)		Xanthine Oxidase Inhibition	
		IC_{50} (nM)	SD	IC_{50} (μM)	SD	IC_{50} (μM)	SD	IC_{50} (μM)	SD
2	BEN	26	3	12.5	1.6	87.6	1.7	22.3	1.1
3	6-OH-BEN	189	9	3.7	0.1	> 100	–	2.3	1.1
4	6-OMe-BEN	111	14	8.9	0.1	43.2	0.4	5.4	1.1
5	6-F-BEN	18	4	39.6	2.7	30.4	2.5	53.3	1.2
6	5-OH-BEN	138	9	11.2	1.1	> 100	–	28.2	1.1
7	5-OMe-BEN	42	9	14.0	0.1	33.8	0.2	47.6	1.1
8	5-F-BEN	6	4	21.1	0.6	18.0	2.2	10.9	1.1
9	5,6-DiF-BEN	245	64	9.7	0.8	17.4	1.7	12.4	1.1
	BEN Compound	**OATP-1B1**		**OATP-1B3**		**OATP-2B1**			
		IC_{50} (μM)	SD	IC_{50} (μM)	SD	IC_{50} (μM)		SD	
2	BEN	1.54	0.51	25.3	4	0.209		0.056	
3	6-OH-BEN	7.78	3.83	6.1	2.5	0.021		0.008	
4	6-OMe-BEN	3.86	0.70	20.9	3.4	8.70		3.6	
5	6-F-BEN	0.73	0.06	ND	ND	0.749		0.077	
6	5-OH-BEN	1.13	0.64	37.6	4.9	0.451		0.165	
7	5-OMe-BEN	2.30	0.72	26.0	4.4	12.2		4.5	
8	5-F-BEN	2.64	0.49	33.4	4.2	0.125		0.031	
9	5,6-DiF-BEN	7.34	1.85	ND	ND	0.135		0.036	

Abbreviation: ND, no data.

hOAT1 and hOAT3 Expressing Oocytes

Analogous experiments were conducted with hOAT1 and hOAT3 expressing oocytes. Probenecid or benzbromarone in the uptake solution displayed (Figures 6 and 7) potent inhibition of [^{14}C]UA uptake. In contrast, when injected inside the

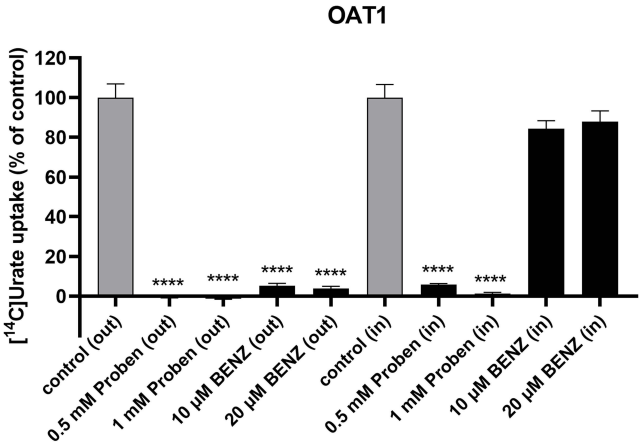

Figure 6 hOAT1 expressing oocytes and urate transport in the presence of either inside or outside probenecid or benzbromarone. ****P<0.0001 vs control, n = 6.

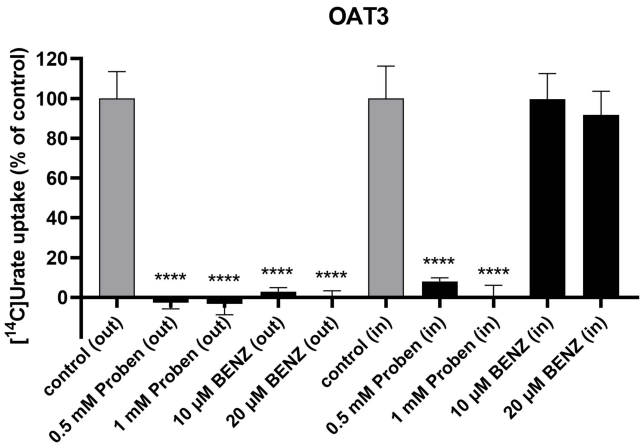

Figure 7 hOAT3 expressing oocytes and urate transport in the presence of either inside or outside probenecid or benzbromarone. ****P<0.0001 vs control, n = 6.

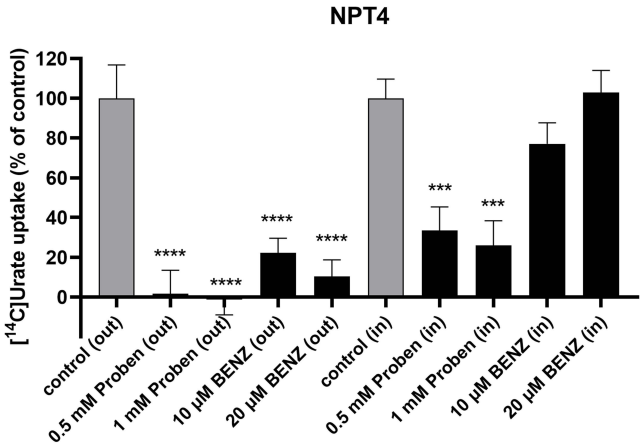

Figure 8 hNPT4 expressing oocytes and urate transport in the presence of either inside or outside probenecid or benzbromarone. ***P<0.001, ****P<0.0001 vs control, n = 6.

oocytes, probenecid displayed potent [^{14}C]UA inhibition, while benzbromarone inside the oocyte did not display a statistically significant difference in [^{14}C]UA uptake. Data illustrates inhibitor site specificity of benzbromarone versus probenecid.

hNPT4 Expressing Oocytes

hNPT4 expressing oocyte experiments were also probed for [^{14}C]UA uptake in the presence and absence of probenecid or benzbromarone. Probenecid or benzbromarone present in the uptake solution displayed (Figure 8) inhibition of [^{14}C]UA uptake; probenecid in the uptake solution displayed a potent [^{14}C]UA decrease in uptake, while benzbromarone was a weak-to-moderate [^{14}C]UA uptake inhibitor. While inside the oocyte, probenecid produced a moderate inhibitory of [^{14}C]UA uptake, while benzbromarone did not produce a statistically significant change in [^{14}C]UA uptake.

Probing the in Vitro Inhibition Kinetics of Benzbromarone and Metabolite, 6-Hydroxy-Benzbromarone

As depicted in Figure 9, Eadie-Hofstee plot and double-reciprocal plot of the Michaelis–Menten equation shows inhibition kinetics from both benzbromarone (**2**) and major metabolite 6-hydroxy-benzbromarone (**3**). These results illustrate that the K_m for [^{14}C]UA uptake was not altered in the presence of **2** or **3**, but rather the V_{max} was reduced in the

https://doi.org/10.2147/DDDT.S474398

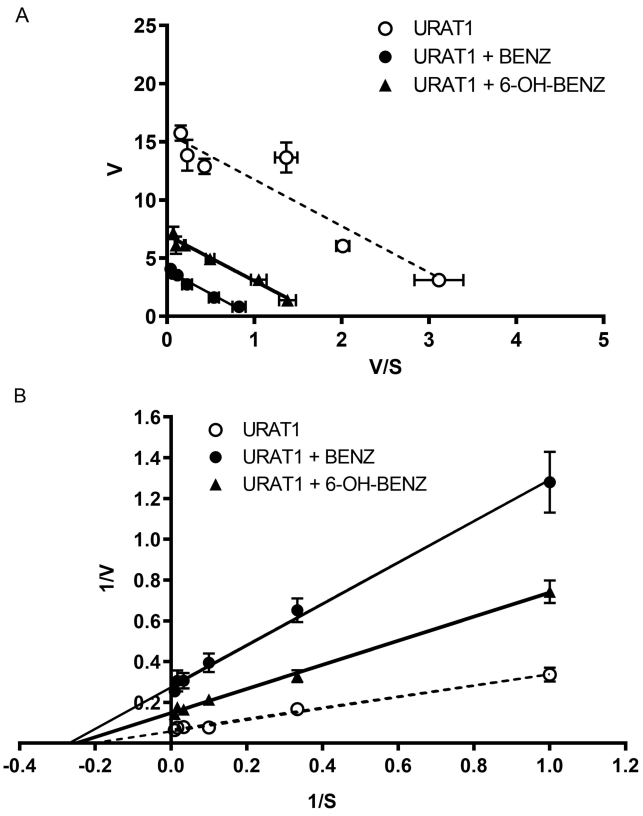

Figure 9 UA inhibition kinetics of 0.1 μM Benzbromarone and 0.3 μM 6-hydroxy benzbromarone; (**A**) Eadie-Hofstee plot and (**B**) double-reciprocal plot of the Michaelis-Menten equation.

presence of inhibitors when added to the uptake solutions. As a result, these data support the notion that **2** and **3** inhibit [^{14}C]UA uptake as non-competitive inhibition and not on the URAT1 binding site.

OATP's Oocytes

As summarized in Table 2, inhibition of the benzbromarone analogs (**2**–**9**) was tested using [^{14}C]UA as the substrate for urate transporters. Whereas in the case of the liver transporters OATPs, the radioactive substrate for 1B1 and 2B1 was [^{3}H]estrone sulfate, while the substrate for 1B3 was [^{3}H]estradiol-17β-glucuronide. These data illustrate i) that the benzbromarone analogs (**2**–**9**) were potent (nM) inhibitors of UA via hURAT1 and ii) that the analogs (**2**–**9**) were not potent UA inhibitors via hOAT10 or hURATv1 (GLUT 9). Furthermore, the analogs were not potent XO inhibitors with metabolite 6-hydroxy-benzbromarone (**3**) being the most potent (IC_{50} 2.3μM) inhibitor of the series and roughly 10-fold more than parent benzbromarone (**2**). Interestingly, we also investigated transporters of the liver (*ie* OATP1B1, OATP1B3 and OAT2B1) utilizing prototypical substrates for 1B1 and 2B1 ([^{3}H]estrone sulfate) and 1B3 ([^{3}H]estradiol-17β-glucuronide). Fluoro analog (**5**) displayed the most potent OATP-1B1 inhibition of 0.73 μM (analog range 0.73–7.78 μM). Metabolite 6-hydroxy-benzbromarone (**3**) was the most potent inhibitor of OATP-1B3 (6.1 μM; analog range 6.1–37.5 μM) and a rather potent OATP-2B1 inhibitor (21 nM; analog range 21–12,200 nM). These data depict the analogs and/or metabolite transporter interactions in the liver. The analogs displayed a range of 0.011–12.2 μM with the methoxy analogs **4** and **7** having high IC_{50} values. The position of the fluorine atom (*ie,* **5** versus **8**) illustrates the importance of the location and electronics, with **8** being a more potent inhibitor.

Rat Pharmacokinetic Study

As summarized in Figure 10A (orbital sinus dosing; 0.43 mg/Kg) and Figure 10B (capsule dosing; 19.6 mg/Kg p.o), the blood versus time profiles for (**5**) are presented. The rat pharmacokinetic results were similar to what was previously

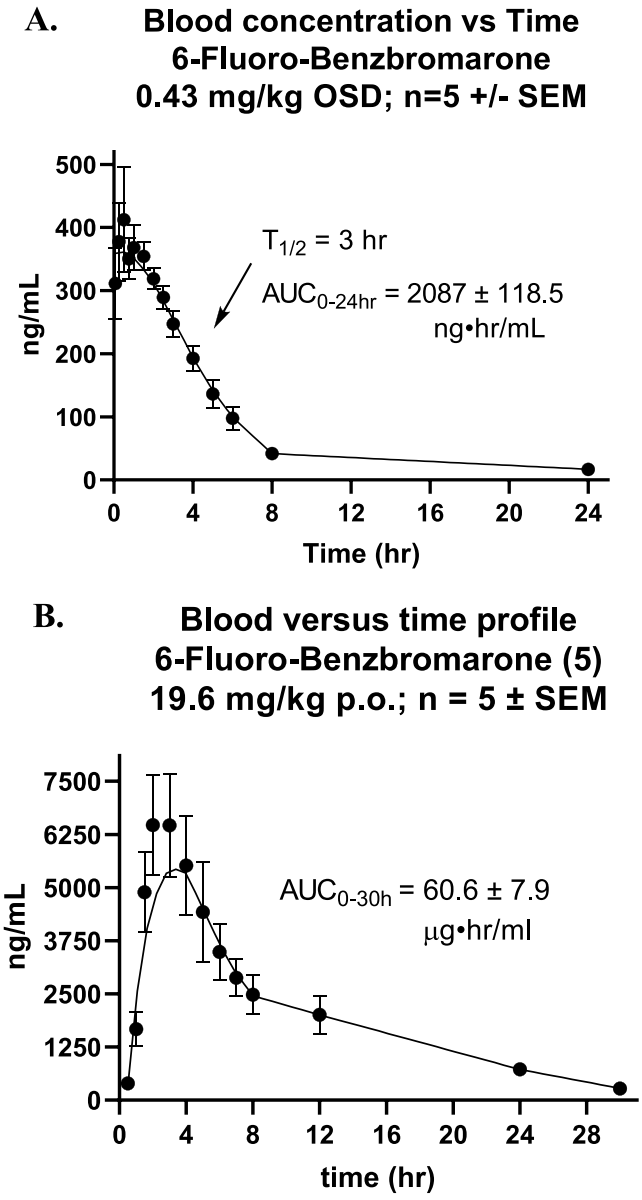

Figure 10 6-fluoro-benzbromarone (**5**) dosed to male Sprague-Dawley rats. (**A**) Orbital sinus dosing (0.42 mg/Kg) and (**B**) Oral capsule dosing (19.6 mg/Kg).

observed for various benzbromarone analogs. Previously, 0.5 mg/kg orbital sinus iv dosing and oral capsule dosing (16–17 mg/kg) was performed.[8] The iv $AUC_{0\text{-}24\ hr}$ data in this study were calculated to be 2087 ± 119 ng•hr/mL; $T_{1/2}$ was essentially 3 hr via iv dose. Herein, the oral capsule dosing (19.6 mg/kg) produced a C_{max} of 6463–6471 ng/mL, with a T_{max} of 2–3 hr and the $AUC_{0\text{-}30hr}$ = 60.6 ± 7.9 µg•hr/mL. The oral bioavailability (F_a) was approximately 0.64 ± 0.04.

Discussion

Previous work in our laboratories described the synthesis of a few benzbromarone analogs (**3**–**5**). In the current work, two additional benzbromarone analogs – 6-fluoro-benzbromarone (**5**) and 5.6-difluoro-benzbromarone (**9**) – were synthetically prepared and tested in vitro. Analog (**5**) was prepared in six synthetic steps starting from 2-fluoro-phenol (**10**); 2.8% overall yield, but reaction conditions were not optimized. Analog (**9**) was prepared in six synthetic steps starting from 2-bromo-4,5-difluorophenol (**16**) in an overall yield of 0.27%. As summarized in Table 1, compound (**5**) had a hURAT1 inhibition of 18 ± 4 nM, while analog (**9**) had an IC_{50} of 245 ± 64 nM. This means that two analogs (**5** and **8**) were found to be more potent than parent benzbromarone (**2**). Analog (**5**) was also administered IV to rats via

https://doi.org/10.2147/DDDT.S474398

orbital sinus dosing (OSD) (n=5 male rats) and oral (capsule) dosing (n=5 male rats). Benzbromarone (**2**) was used as an internal standard in the LC/MS-MS analysis of blood samples. The OSD (0.42 mg/kg) of (**5**) produced a delay in the maximum concentration, which was essentially 0.5 hr post-dose. The OSD $AUC_{0\text{-}24\ hr}$ was calculated to be 2087 ± 119 ng•hr/mL (Figure 10A); $T_{1/2}$ was essentially 3 hr. The oral capsule dosing (19.6 mg/kg) produced a C_{max} of 6463–6471 ng/mL, with a T_{max} of 2–3 hr and the $AUC_{0\text{-}30hr}$ = 60.6 ± 7.9 μg•hr/mL (Figure 10B); the oral bioavailability (F_a) was approximately 0.64 ± 0.04.

Additional research was performed using the oocyte expression system.[9,10] Oocytes expressing hURAT1, hURATv1 (GLUT9), hOAT1, hOAT3, hOAT10, hNPT4, OATP1B1, OATP1B3, and OATP2B1 were prepared. As depicted in Figure 3, apical transporters involved in uric acid transport from the urine/renal tubular cell interface via re-absorption pathways include hURAT1, hOAT10, with excretion via NPT4. In contrast, on the basolateral side, the re-absorption pathway via GLUT9 (hURATv1), while excretion via transporters hOAT1 and hOAT3. Other research groups have also denoted that urate is a substrate for various important drug transporters.[11–14] Our laboratories have investigated drug-transporter interactions via transporter expressing system with both inside and outside drug-transporter interactions. As summarized in Figure 4, hURAT1 ^{14}C-uric acid transport could be inhibited when probenecid (**1**) was added to the incubation media; it displayed a dose-dependent inhibition, albeit at high drug concentrations. Furthermore, when (**1**) was injected into the oocyte, it too showed a dose-dependent inhibition of ^{14}C-uric acid transport. When (**2**) was present in the uptake media, it too showed potent ^{14}C-uric acid transport inhibition. In contrast, unlike (**1**), when (**2**) was injected into the oocyte it did not produce a profound inhibition; some inhibition was observed at the higher drug level but we equate it to (**2**) at 20 μM affords some transport out of the oocyte and thus starts to inhibit ^{14}C-uric acid transport via the outside effect.

As presented in Figure 5, hOAT10 site-specific interactions were probed with probenecid (**1**) and benzbromarone (**2**). When placed in the incubation media, (**1**) displayed a dose-dependent inhibition of ^{14}C-uric acid transport. While compound (**2**) in the incubation media also displayed a dose-dependent effect, it was only roughly 50% of control. In contrast, when (**1**) was injected into the oocyte expression system, it displayed a dose-dependent inhibition of ^{14}C-uric acid transport, whereas (**2**) did not display this effect. The hOAT1 (Figure 6) and hOAT3 (Figure 7) expressing oocytes produced similar results, that is, (**1**) and (**2**) included in the incubation media produces a potent ^{14}C-uric acid transport inhibition. Probenecid (**1**) injected into the oocytes produced a profound inhibition, while (**2**) inside the oocyte was not readily inhibited. Lastly, as summarized in Figure 8, NPT4 expressing oocytes were also investigated to illustrate that (**1**) and (**2**) in the incubation media produced dose-dependent inhibition. When (**1**) and (**2**) were injected into the oocyte, (**1**) produced moderate inhibition which (**2**) did not.

OATP-1B1, OATP-1B3 and OATP-2B1 are important liver drug transporters.[14] OATP expressing oocytes (OATP-1B1, OATP-1B3 and OATP-2B1) were also prepared with [^{3}H]estrone sulfate as the substrate for 1B1 and 2B1, while [^{3}H]estradiol-17β-glucuronide. As summarized in Table 2, the most potent OATP-1B1 inhibitor from the series of analogs was **5** (739 nM), 6-fluoro-benzbromarone, while the other analogs were between 1.1 and 7.8 μM. Regarding OATP-1B3, the analogs were μM inhibitors (6–38 μM) with benzbromarone metabolite (**7**) as the most potent at 6.1 μM; we were unable to obtain OATP1B3 data for the analogs, (**5**) and (**9**). In contrast, OATP-2B1 expressing oocytes displayed more potent inhibition (21 to 749 nM) with the two methoxy analogs (**3**) and (**6**) were far less potent; analog (**7**) was the most potent at 21 nM. Furthermore, the xanthine oxidase inhibitor activity for the analogs ranged from 2.3 to 53.3 μM with the 6-hydroxy-benzbromarone metabolite (**3**) being the most potent analog and also illustrates the importance of the location of the hydroxy group (*ie,* **3** versus **6**).

Lastly, ^{14}C-uric acid transport kinetics of **2** (100 nM) and metabolite **7** (300 nM) were performed to generate Figure 9A (Eadie-Hofstee plot) and Figure 9B (Double-reciprocal plot of the Michaelis–Menten equation). The results demonstrate non-competitive inhibition, which is a form of allosteric regulation at a site different from the active site where the substrate binds and a specific type of inhibitor inhibition results in decreased efficiency of the enzyme.

Conclusion

Since its introduction to inhibit the renal elimination of penicillin, probenecid was recognized as a uricosuric agent which inhibits the renal tubular reabsorption of uric acid, lowering uric acid. Benzbromarone has a different chemical structure

but shares uricosuric activity with probenecid. The current report describes two substituted benzbromarone analogs with good oral bioavailability and improved potency at hURAT1 with positional influence of substitution by -OMe, -OH or -F. Differences between probenecid and benzbromarone and its metabolites and analogs at URAT1, OAT1, OAT3, OAT10 and NPT4 show differences between probenecid and benzbromarone. Results support benzbromarone and its metabolites as noncompetitive inhibitors at hURAT1. Benzbromarone presents a promising framework for molecular modifications that enhance inhibitory activity at uric acid transporters.

Abbreviations

ACN, acetonitrile; F_a, bioavailability; $CaCl_2$, calcium chloride; $Ca(NO_3)_2$, calcium nitrate; CS_2, carbon disulfide; CMC, carboxy-methyl-cellulose; $CDCl_3$, chloroform-$_d$; DCM, dichloromethane; DEG, diethylene glycol; DMSO-d_6, dimethyl-sulfoxide d_6; EtOAc, ethyl acetate; GLUT9, transporter 9 (URATv1; SLC2A9, facilitated glucose transporter member 9; Hex, hexanes; HCl, hydrochloric acid; HEPES, *N*-(2-hydroxyethyl)piperazine-*N*′-(2-ethane sulfonic acid); NPT4, Human Sodium-Phosphate Transporter 4 (hNPT4; SLC17A3); LOD, Limit-of-Detection; LOQ, Limit-of-Quantitation; $MgSO_4$, magnesium sulfate; MeOH, methanol; NMR, nuclear magnetic resonance; OAT, Organic Anion Transporter; OAT1, organic anion transporter 1 (SLC22A6) and OAT3, organic anion transporter 3 (SLC22A8); OAT10, Organic Anion Transporter 10 (human Organic Anion Transporter 10; SLC22A13); OATP1B1, Organic Anion Transporting Polypeptide 1B1; SLCO1B1), OATP1B3 (Organic anion transporting polypeptide 1B3; SLCO1B3), and OATP1B1 (Organic anion transporting polypeptide 2B1; SLCO2B1); OSD, orbital sinus dosing; K_2CO_3, potassium carbonate; KCl, potassium chloride; RBF, Round-Bottom Flask; SB, Stir-Bar; SC, standard curve; SAR, Structure-Activity Relationship; $NaHCO_3$, sodium bicarbonate; NaCl, sodium chloride; SDS, sodium dodecyl sulfate; (Na_2SO_4), sodium sulfate; TEA, triethylamine, THF, tetrahydrofuran; TLC, thin-layer chromatography; UA, Uric Acid; URAT1, Uric acid transporter 1 (SLC22A12); XO, Xanthine Oxidase.

Ethical Approval

The in vivo rat experiments were conducted at East Tennessee State University (ETSU), Quillen College of Medicine (Johnson City, TN). The animal experiments were approved by the Association for Assessment and Accreditation of Laboratory Care International accredited facility. All procedures were reviewed and approved by the ETSU Committee of Animal Care. In addition, the research procedures adhered to the Principles of Laboratory Animal Care (National Institutes of Health (NIH) publication No. 85-23), which was revised in 1985.

Author Contributions

All authors made a significant contribution to the work reported, whether that is in the conception, study design, execution, acquisition of data, analysis and interpretation, or in all these areas; took part in drafting, revising or critically reviewing the article; gave final approval of the version to be published; have agreed on the journal to which the article has been submitted; and gave final approval of the version to be published; have agreed on the journal to which the article has been submitted; and agree to be accountable for all aspects of the work.

Funding

This work was supported by sponsored research agreements via J Pharma Co. LTD (Yokohama, Japan) and East Tennessee State University (ETSU) and the University of Colorado (UCD), School of Pharmacy. In addition, Grant-in-Aid for Research Activity start-up from Japan Society for the Promotion of Science (JSPS) # 21890245, Grant-in-Aid for Scientific Research (C) from JSPS #23590647, #23591205 and #26461258 were used to support the current research.

Disclosure

MFW and HE denote that they are inventors on a patent, US-10005750-B2 and thus have a competing interest. The other authors declare that they have no known competing financial interests or personal relationships that could have appeared to influence the work reported in this paper.

References

1. Enomoto A, Kimura H, Chairoungdua A. et al. Molecular identification of a renal urate anion exchanger that regulates blood urate levels. *Nature*. 2002;417(6887):447–452. doi:10.1038/nature742
2. Schlesinger N. Diagnosing and treating gout: a review to aid primary care physicians. *Postgrad Med.* 2010;122(2):157–161. doi:10.3810/pgm.2010.03.2133.
3. Song D, Zhao X, Wang F, Wang G. A brief review of urate transporter 1 (URAT1) inhibitors for the treatment of hyperuricemia and gout: current therapeutic options and potential applications. *Eur J Pharm*. 2021;907:174291. doi:10.1016/j.ejphar.2021.174291
4. Zhang M-Y, Niu J-Q, Wen X-Y, Jin Q-L. Liver failure associated with benzbromarone: a case report and review of the literature. *World J Clin Cases*. 2019;7(13):1717–1725. doi:10.12998/wjcc.v7.i13.1717
5. Wang H, Peng Y, Zhang T, et al. Metabolic Epoxidation is a critical step for the development of benzbromarone-induced hepatotoxicity. *DMD*. 2017;45(12):1354–1363. doi:10.1124/dmd.117.077818
6. Wempe M, Endou H. Developing potent urate transporter inhibitors: compound designed for their uricosuric action. United States Patent (PCT Filed Oct, 6th, 2011; WO2012/048058) and US 10,005,750 B2, Jun 26th, 2018.
7. Jutabha P, Wempe MF, Anzai N, Otomo J, Kadota T, Endou H. Xenopus laevis oocytes expressing human P-glycoprotein: probing trans- and cis-inhibitory effects on [3H]vinblastine and [3H]digoxin efflux. *Pharmacol Res*. 2010;61(1):76–84. doi:10.1016/j.phrs.2009.07.002
8. Wempe MF, Quade B, Jutabha P, et al. Human uric Acid Transporter 1 (hURAT1): an inhibitor Structure-Activity Relationship (SAR) study. *Nucleosides Nucleotides Nucleic Acids*. 2011;30(12):1312–1323. doi:10.1080/15257770.2011.594031
9. Wempe MF, Lightner JW, Miller B, et al. Potent hURAT1 inhibitors: in vitro and in vivo metabolism and pharmacokinetic studies. *Drug Des Devel Ther*. 2012;6:323–339. doi:10.2147/DDDT.S35805
10. Wempe MF, Jutabha P, Quade B, et al. Developing Potent Human Uric Acid Transporter 1 (hURAT1) inhibitors. *J Med Chem*. 2011;54(8):2701–2713. doi:10.1021/jm1015022
11. Mandal AK, Mount DB. The molecular physiology of uric acid homeostasis. *Annu Rev Physiol*. 2015;77(1):323–325. doi:10.1146/annurev-physiol-021113-170343
12. Xu L, Shi Y, Zhuang S, Liu N. Recent advances on uric acid transporters. *Oncotarget*. 2017;8(59):100852–100862. doi:10.18632/oncotarget.20135
13. Nigam SK, Bhatnagar V. The systems biology of uric acid transporters: the role of remote sensing and signaling. *Curr Opin Nephrol Hypertens*. 2018;27(4):305–313. doi:10.1097/MNH.0000000000000427
14. Sun HL, Wu YW, Bian HG, et al. Function of uric acid transporters and their inhibitors in hyperuricaemia. *Front Pharmacol*. 2021;12:667753. doi:10.3389/fphar.2021.667753